ACSNANO
www.acsnano.org
ARTICLE

Multilayer Transfer Printing for Pixelated, Multicolor Quantum Dot Light-Emitting Diodes

Bong Hoon Kim,[†] Sooji Nam,[†] Nuri Oh,[†] Seong-Yong Cho,[†] Ki Jun Yu,[†] Chi Hwan Lee,[‡] Jieqian Zhang,[§] Kishori Deshpande,[∥] Peter Trefonas,[§] Jae-Hwan Kim,[†] Jungyup Lee,[†] Jae Ho Shin,[†] Yongjoon Yu,[†] Jong Bin Lim,[†] Sang M. Won,[†] Youn Kyoung Cho,[†] Nam Heon Kim,[†] Kyung Jin Seo,[†] Heenam Lee,[†] Tae-il Kim,[⊥] Moonsub Shim,*[,†] and John A. Rogers*[,†]

[†]Department of Materials Science and Engineering, Beckman Institute for Advanced Science and Technology, Frederick Seitz Materials Research Laboratory, University of Illinois at Urbana−Champaign, Urbana, Illinois 61801, United States

[‡]Weldon School of Biomedical Engineering, School of Mechanical Engineering, The Center for Implantable Devices, and Birck Nanotechnology Center, Purdue University, West Lafayette, Indiana 47907, United States

[§]Dow Electronic Materials, 455 Forest Street, Marlborough, Massachusetts 01752, United States

[∥]The Dow Chemical Company, 2301 North Brazosport Boulevard, Freeport, Texas 77541, United States

[⊥]Center for Neuroscience Imaging Research (CNIR), Institute of Basic Science (IBS); School of Chemical Engineering, Sungkyunkwan University (SKKU), Suwon 440-746, Korea

Supporting Information

ABSTRACT: **Here, we report multilayer stacking of films of quantum dots (QDs) for the purpose of tailoring the energy band alignment between charge transport layers and light emitting layers of different color in quantum dot light-emitting diodes (QD LED) for maximum efficiency in full color operation. The performance of QD LEDs formed by transfer printing compares favorably to that of conventional devices fabricated by spin-casting. Results indicate that zinc oxide (ZnO) and titanium dioxide (TiO_2) can serve effectively as electron transport layers (ETLs) for red and green/blue QD LEDs, respectively. Optimized selections for each QD layer can be assembled at high yields by transfer printing with sacrificial fluoropolymer thin films to provide low energy surfaces for release, thereby allowing shared common layers for hole injection (HIL) and hole transport (HTL), along with customized ETLs. This strategy allows cointegration of devices with heterogeneous energy band diagrams, in a parallelized scheme that offers potential for high throughput and practical use.**

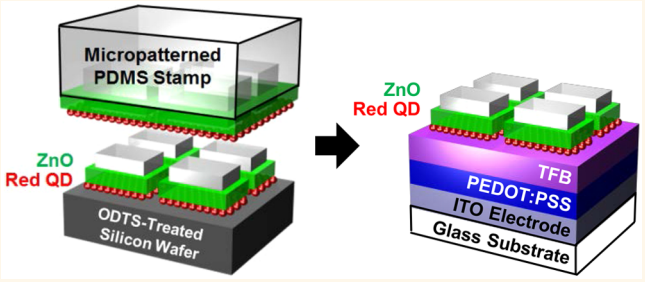

KEYWORDS: *quantum dots, light-emitting diode, transfer printing, energy band diagram*

Chemically synthesized colloidal semiconductor quantum dots (QDs) are of interest for applications in electronics and optoelectronics due to their unique properties including size dependent band structure.[1−7] Advanced solution-phase synthesis techniques enable not only routes to uniform QDs and even complex quantum heterostructures but also simple solution-casting methods for utilizing these materials in passive and active device structures.[8−14] Light emitting diodes that incorporate solution processed films of QDs (i.e., QD LEDs) as emissive layers are of particular interest due to rapid progress in performance, with levels of efficiency that are comparable to those of organic LEDs.[15−17] Energy band alignment between the charge transport layers and QDs in these devices is critically important to their operation.[18−21] For example, hole transport materials with low HOMO levels enable improved hole injection into QDs due to the low band offset. Electron injection that occurs at the interface between the ETL and the QDs can be considered in the same manner as that for hole injection.[17,22] Inorganic materials, especially metal oxides such as ZnO, TiO_2, SnO_2, exhibit better band alignment with QDs than that possible with organic materials that have been explored to date.[18−21] Well-matched energy levels increase the energy

Received: October 10, 2015
Accepted: April 14, 2016

DOI: 10.1021/acsnano.5b06387
ACS Nano XXXX, XXX, XXX−XXX

conversion efficiency and lower the threshold voltages for operation.[17,23,24] Of special note are QD LEDs with hybrid organic–inorganic HTLs and ETLs formed by spin-casting, in ways that maintain high performance by tailored band alignment.[8,17]

Although such solution processing routes are attractive, the formation of complex, multilayer assemblies is constrained by the need to avoid redissolution of existing layers during the deposition of overcoats. In addition, although recent work suggests promise for emerging methods based on electrohydrodynamic jet printing,[25−27] established techniques based on screen printing and ink jet printing do not offer levels of resolution needed for high performance displays. Recent advances in dry processing approaches generally, and transfer printing[28] in particular, suggest powerful capabilities in this context, wherein quantum dots can be patterned for each color component in a display, in a rapid, parallel process with micron and submicron resolution.[29−32] Here, direct physical transfer of materials occurs from soft flexible stamps to enable formation of isolated structures of QD films on a target substrate for pixelated QD LEDs. Difficulties in the patterned deposition of other device layers, however, remain. Although transfer printing may provide a solution for these cases as well, the surface properties of each layer must be considered carefully to ensure adequate adhesive interactions for high-yield transfer.[30,31]

In this paper, we present a scheme for multilayer transfer printing in which a thin film of a fluoropolymer serves as a low energy protective coating on the top surface of a preformed stack that includes an emissive layer, charge transport layer, and metal electrode, optimized in terms of the energy band diagrams. After transfer, the fluoropolymer can be easily removed without affecting the other layers due to its unique orthogonal solvent properties. Although many combinations are possible, we focus on fabrication of QD LEDs with shared common layers of HIL and HTL and customized ETLs. ETLs tailored to the band gap of each type of QD layer[33−36] in a pixelated, multicolor array can be printed in this manner. This strategy offers versatile capabilities in the fabrication of full color QD LEDs where the ETLs in each color pixel have energy band alignments designed to maximize EQE and luminance, regardless of the lateral geometries of the patterned active QD layers.

RESULTS AND DISCUSSION

Figure 1 presents a schematic illustration of the multilayer transfer process performed with a polydimethylsiloxane (PDMS) elastomeric stamp and a fluoropolymer as an antiadhesive capping layer. It also shows top view optical micrographs at each step. The process begins with the preparation of a donor substrate that consists of a silicon wafer functionalized with a self-assembled monolayer of octadecyltrichlorosilane (ODTS) on its surface to minimize adhesion. Spin-casting 30 nm thick CdSe/CdS/ZnS core–shell red QDs and 25 nm thick zinc oxide (ZnO, ETL) from sol-gel solution and thermally annealing (90 °C for 20 min, 110 °C for 30 min in vacuum) forms the functional layers on this substrate. Electron beam evaporation through a shadow mask yields a 100 nm thick aluminum (Al) electrode to complete the multilayer stack (Figure 1a). Contact and removal of the stamp peels away selected regions of this stack to leave pixelated patterns in the desired geometry. The geometry of the relief on the stamp defines the pixel dimensions in this subtractive form of transfer printing (Figure 1b). Next, a thin film of a fluoropolymer (1

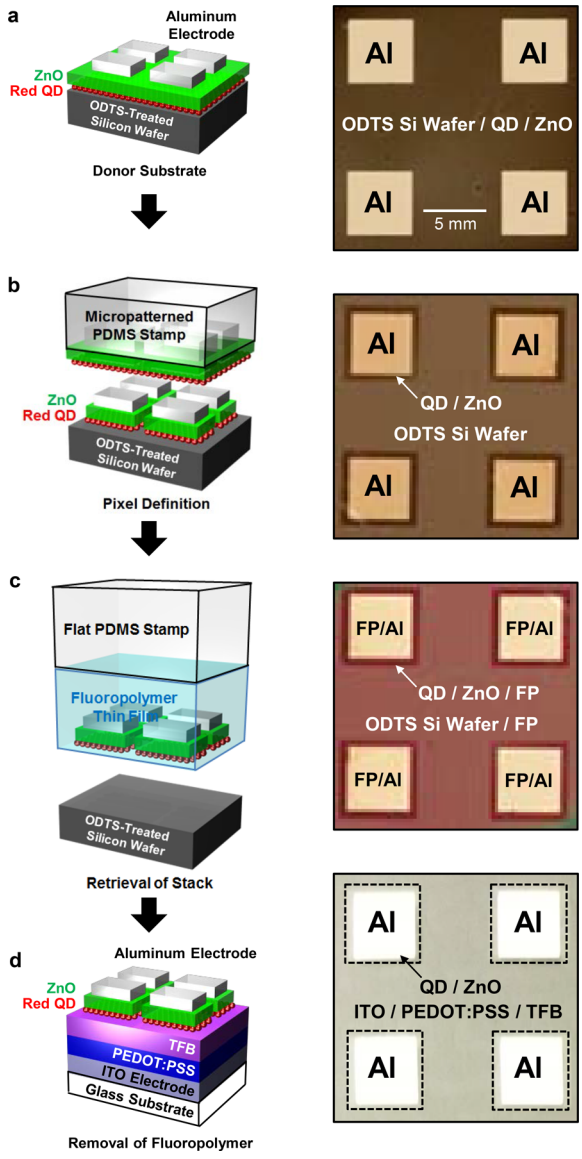

Figure 1. Schematic illustration of a process for multilayer transfer printing of active materials for QD LEDs and top view optical micrographs corresponding to each step. (a) Sequential spin-coating steps and thermal annealing define films of CdSe/CdS/ZnS core–shell red QDs and zinc oxide (ZnO) on an ODTS-treated silicon substrate. Electron beam evaporation through a shadow mask defines aluminum (Al) electrodes. (b) Contacting and removing a PDMS stamp peels away selected regions of the multilayer stack to leave pixelated patterns in the desired geometry. (c) Spin-casting and thermal annealing forms a thin film of a fluoropolymer material over the pixelated QD/ZnO/Al structures. A flat PDMS stamp provides a means to retrieve the fluoropolymer layer with the pixel structures on its surface, for delivery to a target substrate. (d) Pixel arrays printed onto a receiver substrate (TFB/PEDOT:PSS/ITO/glass) followed by solvent removal of the fluoropolymer yield functional devices.

μm, OSCoR 2312 photoresist solution, Orthogonal INC) spin-cast on the pixelated QD/ZnO/Al and then thermally annealed (100 °C for 1 min) yields a low energy coating (about 35 mJ/m^2). Retrieval of the resulting pixelated stacks, all embedded in the fluoropolymer layer, occurs with a flat PDMS stamp. Adhesion to the fluoropolymer is sufficiently strong to allow retrieval of the multilayers (QD/ZnO/Al/fluoropolymer) from

DOI: 10.1021/acsnano.5b06387
ACS Nano XXXX, XXX, XXX–XXX

the donor substrate, but is sufficiently weak to enable release onto a target substrate (Figure 1c and Figure S1). Advantages of use of the fluoropolymer include: (i) the introduction of carrier to facilitate retrieval of pixels onto the flat PDMS stamp at yields that are consistently 100% (Figure S2) and (ii) the entire array of pixels transfers in a single retrieval and delivery step. The low surface energy and the orthogonal solvent properties of the fluoropolymer are key to its use in this context.

Transfer of the QD/ZnO/Al/fluoropolymer stack occurs at elevated temperatures (100 °C for 10 min; Figure 1d) onto a glass substrate that supports a prepatterned, 150 nm thick indium tin oxide (ITO) anode (cleaned with acetone/isopropyl alcohol (IPA)/DI water and exposed to UV Ozone (UVO) for 10 min) with a spin-cast and thermally annealed (210 °C for 10 min) 40 nm thick hole injection layer (HIL) of poly(3,4-ethylenedioxythiophene)polystyrenesulfonate (PEDOT:PSS). A spin-cast and thermally annealed (180 °C for 30 min) 20 nm thick film of poly[(9,9-dioctylfluorenyl-2,7-diyl)-*co*-(4,40-(*N*-(4-*s*-butylphenyl)) diphenylamine)] (TFB) solution serves as the hole transfer layer (HTL). The final step involves immersion in a stripper solution (Orthogonal stripper 700 solution, Orthogonal INC) to remove fluoropolymer, without any measurable effect on the underlying layers (Figure S3).[37]

Processing steps that follow previously reported procedures yield QD LEDs from these transferred multilayers.[30,38] Figure 2a and b show photographs of working devices at operation voltages of 4 V, along with the electroluminescence (EL) spectra of green (EL = 536 nm) and red (EL = 628 nm) QD LEDs. Both types of devices exhibit narrow EL peaks (full width at half-maximum < 50 nm) with no parasitic emission from the HTL or ETL (Figure 2c). Figures 2d–f present the performance compared to otherwise similar devices formed by the sequential spin-casting. The relative current density–voltage (J–V), the maximum luminance–voltage (L–V) and the external quantum efficiency (EQE) characteristics of devices (Figure 2e and f, red line) formed by transfer are comparable to or slightly better than conventional devices (Figure 2e and f, black line).

The main attractive feature of the transfer scheme is that it enables patterned delivery of materials for individual red–green–blue QDs onto a single target substrate.[29−31] The multilayer approach reported here builds on this advantage by allowing the use of different material stacks for LEDs with different colors. We characterized QD LEDs that include HIL/HTL layers of PEDOT:PSS/TFB/(red, green, or blue QDs)/(ZnO or TiO_2)/Al, where QDs and ETL are separately selected to maximize performance. Figure 3a–d and Figure S4 show the characteristics of red, green or blue QD LEDs with different ETL materials (i.e., ZnO or TiO_2). Previous reports[30,38] provide guidance on the selection of the thicknesses of the ZnO and TiO_2. Red QD LEDs (Figure 3a and b) that use ZnO exhibit maximum luminance values at 10 V, more than 1 order of magnitude higher than otherwise identical devices formed with TiO_2. The ZnO also enables much higher maximum EQE than TiO_2 (Figures S5 and S6). By contrast, green QD LEDs show the opposite trends (Figure 3c and d): although the maximum luminances of green QD LEDs with ZnO and TiO_2 are similar, the maximum EQE enabled by TiO_2 is greater than that by ZnO. The results in Figure S4 shows that blue QD LEDs with TiO_2 exhibit characteristics better than those with ZnO.

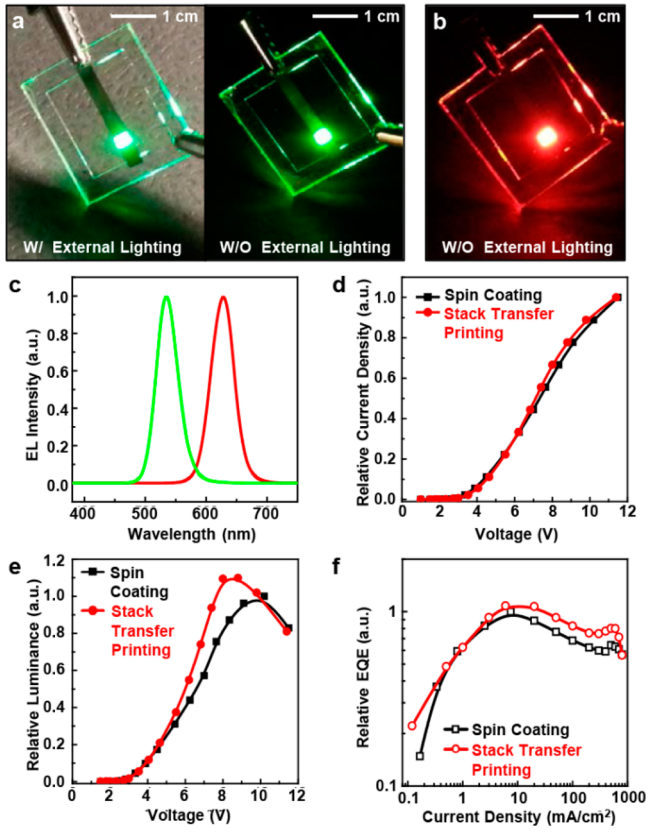

Figure 2. Photographs of transfer printed (a) green and (b) red QD LEDs at an operation voltage of 4 V. (c) Electroluminescence (EL) spectra of the corresponding green (EL = 536 nm) and red (EL = 628 nm) QD LEDs. Performance ((d) current density–voltage, (e) luminance–voltage, and (f) external quantum efficiency) of the conventional (black curves) and transfer printed (red curves) red QD LEDs.

Figure 3e, f, and g provide schematic illustrations of the energy band alignment between charge transport layers and QDs having different band gaps and energy levels. The band edge positions of the ETLs (ZnO and TiO_2) are based on band energies relative to the vacuum level experimentally measured via ultraviolet photoelectron spectroscopy (UPS). Absorption spectra provide the optical band gaps (Figure S7). The energy level of the conduction band edge of ZnO is similar to the work function of Al, that is, 4.3 eV. The conduction level of TiO_2 is ~3.9 eV, which might create a barrier to electron injection from the electrode. The relatively small band offset is expected to make ZnO more suitable for the electron injection than TiO_2. In addition, ZnO can facilitate electron migration toward the red QDs due to the ideal band alignment for charge injection (Figure 3f). However, the band alignment of ZnO with green and blue QDs may be less than ideal due to the large conduction band offset and associated hindrance for electron injection into the QDs (Figure 3g). In contrast, the conduction band edge of TiO_2 lies between those of the green and blue QDs and the Al electrode. The well-aligned TiO_2 energy level results in improved electron transfer into the green or blue QDs compared to ZnO. Multilayer transfer printing provides a practical path for exploiting this type of separate engineering of band alignment for different colored QD LEDs in a pixelated array.

DOI: 10.1021/acsnano.5b06387
ACS Nano XXXX, XXX, XXX–XXX

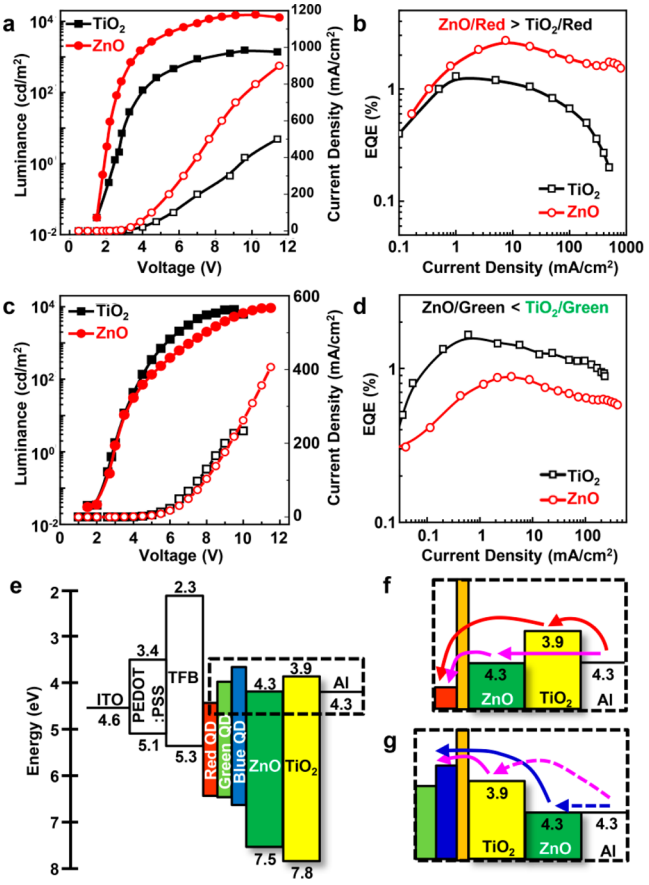

Figure 3. Current density−voltage, luminance−voltage, and external quantum efficiency of red ((a) and (b)) and green ((c) and (d)) QD LEDs with different ETL (ZnO or TiO_2). (e) Schematic illustration of the energy band alignment between charge transport layers (ZnO and TiO_2) and QDs (red, green, and blue) with different band gaps and energy levels. Energy band diagrams of (f) "red QD with ZnO or TiO_2" and (g) "green/blue QD with ZnO or TiO_2".

Figure 4 shows that multilayer transfer enables integration on a single substrate in which the red and green QDs pixels incorporate different, optimized HTLs. TiO_2/green QDs pixel array embedded in fluoropolymer layer was prepared with same technique explained in Figure 1 and transferred on the receiver substrate (TFB/PEDOT:PSS/ITO/glass) (Figure 4a and b). Then, ZnO/red QDs pixel array was printed while aligned between TiO_2/green QDs pixel array (Figure 4c and Figure S8). Figure 4d and e show fluorescence microscopy (FOM) images of receiver substrate after printing TiO_2/green QD pixel array and, subsequently, printing ZnO/red QD pixel array. In conclusion, it is demonstrated that each red and green QD pixel can have a different ETL material and the same kind of HTL on the same substrate (Figure S9). This approach has significant implications in that the device performance of Cd-free QD LEDs is deeply related to its electron transfer layer (ETL), whereas the hole injection layer (HTL) is still limiting factor in the case of conventional Cd-based QD LEDs.[39]

CONCLUSION

The results presented here establish multilayer transfer printing as a route to high efficiency of QD LEDs with the tailored energy band diagram. Multilayer assemblies prepared on donor substrates can be successfully transferred to receiver substrates

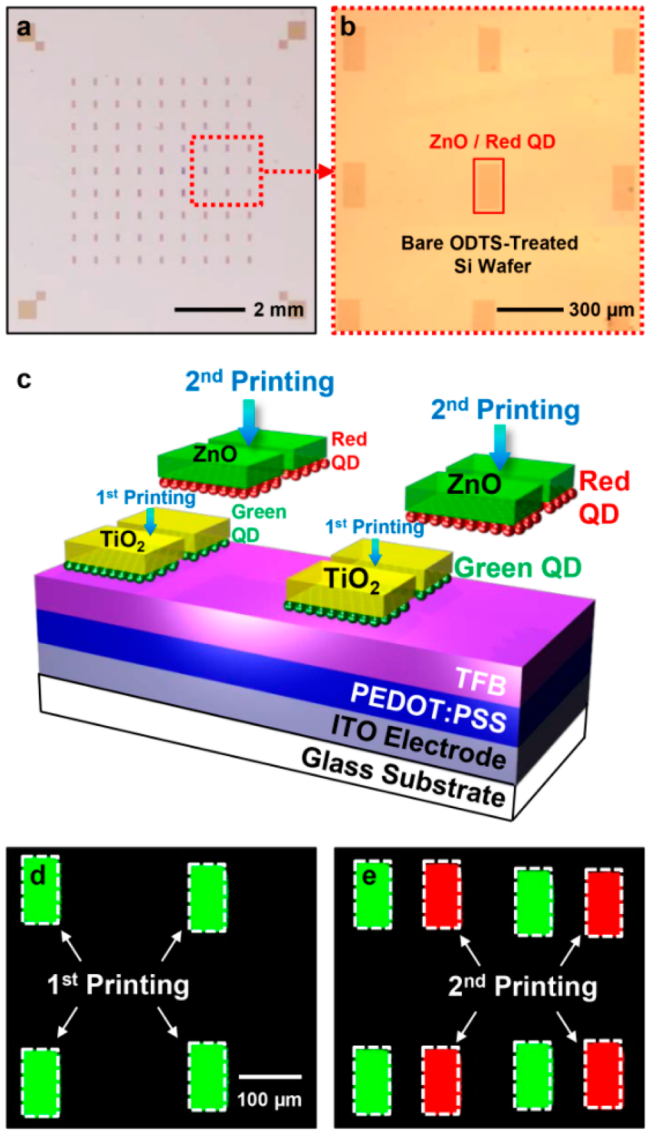

Figure 4. Optical micrographs ((a) and (b)) of pixelated arrays of ZnO/red QDs on an ODTS-treated silicon wafer, patterned by a subtractive process using a PDMS stamp. (c) Schematic illustration of ZnO/red QDs and TiO_2/green QDs pixels delivered to the same substrate by multilayer transfer printing. Fluorescence microscopy (FOM) images of the substrate (d) after printing green pixel array and (e) subsequently printing red pixel array.

regardless of the number of layers. A key advance involves the introduction of a hydrophobic fluoropolymer thin film, which facilitates the process and is easily eliminated without damage to the QD LED after transfer. In this manner, it is possible to create pixelated arrays of QDLEDs with heterogeneous energy band diagrams, with well-matched HOMO/LUMO level between the charge transport layer, charge injection layer, and active layer. These results have potential relevance to a variety of optoelectronic[40−42] and electronic devices,[43−45] especially those fabricated by solution processes, on the same substrate.

METHODS

Quantum Dot Synthesis. *Chemicals.* The reactions were carried out in a standard Schlenk line under N_2 atmostsphere. Technical grade trioctylphosphine oxide (TOPO) (90%), technical grade trioctylphos-

DOI: 10.1021/acsnano.5b06387
ACS Nano XXXX, XXX, XXX−XXX

phine (TOP) (90%), technical grade octylamine (OA) (90%), technical grade trioctylamine (TOA) (90%), technical grade octadecene(ODE) (90%), CdO (99.5%), Zn acetate (99.99%), S powder (99.998%), and Se powder (99.99%) were obtained from Sigma-Aldrich. ACS grade chloroform and methanol were obtained from Fischer Scientific. All chemicals were used as received.

Synthesis of Red Quantum Dots. Red CdSe/CdS/ZnS were prepared in a manner similar to established methods.[33] A total of 1.6 mmol of CdO powder (0.206 g), 6.4 mmol of OA, and 40 mL of TOA in a 200 mL three-neck round-bottom flask were degassed at 150 °C for 30 min under vacuum. Then, the solution was heated to 300 °C under N_2 atmosphere. At 300 °C, 0.4 mL of 1.0 M TOP:Se, previously prepared in glovebox, was swiftly injected into the Cd-containing reaction mixture. After 45 s, 1.2 mmol of *n*-octanethiol dissolved in 6 mL of TOA was slowly injected at a rate of 1 mL min^{-1} via a syringe pump. The reaction mixture was then allowed to stir for an additional 30 min at 300 °C. Simultaneously, 16 mL of 0.25 M Zn-oleate solution dissolved in TOA was prepared in a separate reaction flask with Zn acetate. The Zn-oleate solution was slowly injected into the CdSe reaction flask, followed by injection of 6.4 mmol of *n*-octanethiol dissolved in 6 mL of TOA at a rate of 1 mL min¯1 using a syringe pump.

Synthesis of Green Quantum Dots. Green CdSe@ZnS (gradient composition shell) quantum dots were prepared in a manner similar to established methods.[34] A total of 0.2 mmol of CdO, 4 mmol of Zn acetate, 4 mmol of OA, and 15 mL of ODE were prepared in a 100 mL three-neck round-bottom flask, degassed at 120 °C for 30 min under vacuum. The solution was heated to 300 °C under N_2 atmosphere. At 300 °C, 0.1 mmol of Se and 3.5 mmol of Se dissolved in 2 mL of TOP was swiftly injected into the reaction flask using a syringe. The reaction solution was then allowed to stir for an additional 10 min at 300 °C before being rapidly cooled by an air jet.

Synthesis of Blue Quantum Dot. Blue ZnCdSSe/ZnS (alloy core with ZnS shell) quantum dots were prepared in a manner similar to established methods.[35] A total of 1 mmol of CdO, 10 mmol of Zn acetate, 7 mL of OA, and 15 mL of ODE were prepared in a 100 mL three-neck round-bottom flask. After degassing these chemicals at 120 °C for 30 min under vacuum, the reaction flask was heated to 300 °C. Then, 2 mmol of S dissolved in 3 mL of ODE was swiftly injected into the reaction flask. After 10 min, 8 mmol of S dissolved in 3 mL of TBP was injected into the reaction flask, and then the reaction temperature was maintained at 300 °C for 30 min. Finally, the reaction solution was cooled to room temperature.

QD LED Device Fabrication. For the spin-coated QD LEDs, the devices were fabricated on ITO-coated glass substrates (sheet resistance of 15−25 Ω/□). The prepatterned ITO substrates were cleaned with acetone and isopropanol, consecutively, and then treated with UV-ozone for 15 min. PEDOT:PSS (Clevios P VP AI 4083) was spin-coated onto the ITO at 4000 rpm and baked at 120 °C for 5 min in air and 180 °C for 15 min in a glovebox. Then TFB (H.W. Sands Corp.) was spin-coated using *m*-xylene (0.5 mg/mL) at 3000 rpm, followed by baking at 180 °C for 30 min in a glovebox. After washing twice with a chloroform and methanol mixture (1:1 volume ratio), QDs were finally dispersed in chloroform solution (~30 mg/mL), and spin-cast on top of the TFB layer at 2000 rpm and then subsequently annealed at 180 °C for 30 min. ZnO or TiO_2 (Sigma-Aldrich) (30 mg/mL in butanol for ZnO and 5 wt % in butanol for TiO_2) was spin-coated at 3000 rpm and annealed at 100 °C for 30 min. ZnO nanoparticles were synthesized following the literature.[36] In brief, a solution of potassium hydroxide (1.48 g) in methanol (65 mL) was added to zinc acetate dihydrate (2.95 g) in methanol (125 mL) solution and the reaction mixture was stirred at 60 °C for 2 h. The mixture was then cooled to room temperature and the precipitate was washed twice with methanol. After ETL spin-casting, a 100 nm thick Al cathode was deposited by an electron-beam evaporator at a rate of 1 Å/s. Finally, the devices were encapsulated using a cover glass with epoxy (NOA 86) in a glovebox.

QD LED Device Characterization. The device characteristics and EL spectra were recorded using a Spectrascan PR-655 spectrophotometer coupled with a Keithely 2602B voltage and current source measurement unit. EQE can be calculated by the ratio of the number of photons emitted by the device to the number of electrons injected. All device measurements were performed under air ambient conditions.

ASSOCIATED CONTENT

Supporting Information

The Supporting Information is available free of charge on the ACS Publications website at DOI: 10.1021/acsnano.5b06387.

Details of adhesion at the fluoropolymer/ODTS-treated Si wafer interface and fluoropolymer/PDMS interface, multilayer pickup and printing yield, AFM images of multilayer, device performance of blue QD LED with ZnO/TiO_2 layer, maximum EQE of QD LEDs with different ETLs, lifetime measurement on red C/S QD LED, UPS data, and UV−visible spectroscopy of ZnO/TiO_2 layer, multilayer transfer printing technique for the integration of small pixel of "red QD/ZnO" and "green QD/TiO_2", and IV characteristics of red/green QD LEDs in small pixel geometries. (PDF)

AUTHOR INFORMATION

Corresponding Authors

*E-mail: mshim@illinois.edu.

*E-mail: jrogers@illinois.edu.

Author Contributions

(B.H.K, S.N., and N.O.) These authors contributed equally.

Notes

The authors declare no competing financial interest.

ACKNOWLEDGMENTS

This material is based on work supported by The Dow Chemical Company.

REFERENCES

(1) Yin, Y.; Talapin, D. The Chemistry of Functional Nanomaterials. *Chem. Soc. Rev.* **2013**, *42*, 2484−2487.

(2) Talapin, D. V. Nanocrystal Solids: A Modular Approach to Materials Design. *MRS Bull.* **2012**, *37*, 63−71.

(3) Norris, D. J.; Efros, A. L.; Erwin, S. C. Doped Nanocrystals. *Science* **2008**, *319*, 1776−1779.

(4) Cargnello, M.; Doan-Nguyen, V. V. T.; Gordon, T. R.; Diaz, R. E.; Stach, E. A.; Gorte, R. J.; Fornasiero, P.; Murray, C. B. Control of Metal Nanocrystal Size Reveals Metal-Support Interface Role for Ceria Catalysts. *Science* **2013**, *341*, 771−773.

(5) Shevchenko, E. V.; Talapin, D. V.; Kotov, N. A.; O'Brien, S.; Murray, C. B. Structural Diversity in Binary Nanoparticle Superlattices. *Nature* **2006**, *439*, 55−59.

(6) Talapin, D. V.; Shevchenko, E. V.; Bodnarchuk, M. I.; Ye, X.; Chen, J.; Murray, C. B. Quasicrystalline Order in Self-Assembled Binary Nanoparticle Superlattices. *Nature* **2009**, *461*, 964−967.

(7) Urban, J. J.; Talapin, D. V.; Shevchenko, E. V.; Kagan, C. R.; Murray, C. B. Synergism in Binary Nanocrystal Superlattices Leads to Enhanced P-Type Conductivity in Self-Assembled PbTe/Ag2 Te Thin Films. *Nat. Mater.* **2007**, *6*, 115−121.

(8) Oh, N.; Nam, S.; Zhai, Y.; Deshpande, K.; Trefonas, P.; Shim, M. Double-Heterojunction Nanorods. *Nat. Commun.* **2014**, *5*, 3642.

(9) Tisdale, W. A.; Williams, K. J.; Timp, B. A.; Norris, D. J.; Aydil, E. S.; Zhu, X.-Y. Hot-Electron Transfer from Semiconductor Nanocrystals. *Science* **2010**, *328*, 1543−1547.

(10) Oh, S. J.; Berry, N. E.; Choi, J.-H.; Gaulding, E. A.; Lin, H.; Paik, T.; Diroll, B. T.; Muramoto, S.; Murray, C. B.; Kagan, C. R. Designing High-Performance PbS and PbSe Nanocrystal Electronic Devices through Stepwise, Post-Synthesis, Colloidal Atomic Layer Deposition. *Nano Lett.* **2014**, *14*, 1559−1566.

DOI: 10.1021/acsnano.5b06387
ACS Nano XXXX, XXX, XXX−XXX

(11) Oh, S. J.; Berry, N. E.; Choi, J.-H.; Gaulding, E. A.; Paik, T.; Hong, S.-H.; Murray, C. B.; Kagan, C. R. Stoichiometric Control of Lead Chalcogenide Nanocrystal Solids to Enhance Their Electronic and Optoelectronic Device Performance. *ACS Nano* **2013**, *7*, 2413−2421.
(12) Leschkies, K. S.; Beatty, T. J.; Kang, M. S.; Norris, D. J.; Aydil, E. S. Solar Cells Based on Junctions between Colloidal PbSe Nanocrystals and Thin ZnO Films. *ACS Nano* **2009**, *3*, 3638−3648.
(13) Zhao, N.; Osedach, T. P.; Chang, L.-Y.; Geyer, S. M.; Wanger, D.; Binda, M. T.; Arango, A. C.; Bawendi, M. G.; Bulovic, V. Colloidal PbS Quantum Dot Solar Cells with High Fill Factor. *ACS Nano* **2010**, *4*, 3743−3752.
(14) Talapin, D. V.; Murray, C. B. PbSe Nanocrystal Solids for N- and P-Channel Thin Film Field-Effect Transistors. *Science* **2005**, *310*, 86−89.
(15) Shirasaki, Y.; Supran, G. J.; Bawendi, M. G.; Bulović, V. Emergence of Colloidal Quantum-Dot Light-Emitting Technologies. *Nat. Photonics* **2012**, *7*, 13−23.
(16) Talapin, D. V.; Lee, J.-S.; Kovalenko, M. V.; Shevchenko, E. V. Prospects of Colloidal Nanocrystals for Electronic and Optoelectronic Applications. *Chem. Rev.* **2010**, *110*, 389−458.
(17) Nam, S.; Oh, N.; Zhai, Y.; Shim, M. High Efficiency and Optical Anisotropy in Double-Heterojunction Nanorod Light-Emitting Diodes. *ACS Nano* **2015**, *9*, 878−885.
(18) Caruge, J. M.; Halpert, J. E.; Wood, V.; Bulović, V.; Bawendi, M. G. Colloidal Quantum-Dot Light-Emitting Diodes with Metal-Oxide Charge Transport Layers. *Nat. Photonics* **2008**, *2*, 247−250.
(19) Caruge, J.-M.; Halpert, J. E.; Bulović, V.; Bawendi, M. G. NiO as an Inorganic Hole-Transporting Layer in Quantum-Dot Light-Emitting Devices. *Nano Lett.* **2006**, *6*, 2991−2994.
(20) Wood, V.; Panzer, M. J.; Halpert, J. E.; Caruge, J.-M.; Bawendi, M. G.; Bulović, V. Selection of Metal Oxide Charge Transport Layers for Colloidal Quantum Dot LEDs. *ACS Nano* **2009**, *3*, 3581−3586.
(21) Chuang, C.-H. M.; Brown, P. R.; Bulović, V.; Bawendi, M. G. Improved Performance and Stability in Quantum Dot Solar Cells through Band Alignment Engineering. *Nat. Mater.* **2014**, *13*, 796−801.
(22) Ho, M. D.; Kim, D.; Kim, N.; Cho, S. M.; Chae, H. Polymer and Small Molecule Mixture for Organic Hole Transport Layers in Quantum Dot Light-Emitting Diodes. *ACS Appl. Mater. Interfaces* **2013**, *5*, 12369−12374.
(23) Mashford, B. S.; Stevenson, M.; Popovic, Z.; Hamilton, C.; Zhou, Z.; Breen, C.; Steckel, J.; Bulovic, V.; Bawendi, M.; Coe-Sullivan, S.; Kazlas, P. T. High-Efficiency Quantum-Dot Light-Emitting Devices with Enhanced Charge Injection. *Nat. Photonics* **2013**, *7*, 407−412.
(24) Yang, Y.; Zheng, Y.; Cao, W.; Titov, A.; Hyvonen, J.; Manders, J. R.; Xue, J.; Holloway, P. H.; Qian, L. High-Efficiency Light-Emitting Devices Based on Quantum Dots with Tailored Nanostructures. *Nat. Photonics* **2015**, *9*, 259−266.
(25) Kim, B. H.; Onses, M. S.; Lim, J.; Nam, S.; Oh, N.; Kim, H.; Yu, K. J.; Lee, J. W.; Kim, J.-H.; Kang, S.-K.; Lee, C. H.; Lee, J.; Shin, J. H.; Kim, N. H.; Leal, C.; Shim, M.; Rogers, J. A. High-Resolution Patterns of Quantum Dots Formed by Electrohydrodynamic Jet Printing for Light-Emitting Diodes. *Nano Lett.* **2015**, *15*, 969−973.
(26) Kress, S. J. P.; Richner, P.; Jayanti, S. V.; Galliker, P.; Kim, D. K.; Poulikakos, D.; Norris, D. J. Near-Field Light Design with Colloidal Quantum Dots for Photonics and Plasmonics. *Nano Lett.* **2014**, *14*, 5827−5833.
(27) Onses, M. S.; Sutanto, E.; Ferreira, P. M.; Alleyne, A. G.; Rogers, J. A. Printing: Mechanisms, Capabilities, and Applications of High-Resolution Electrohydrodynamic Jet Printing. *Small* **2015**, *11*, 4412.
(28) Carlson, A.; Bowen, A. M.; Huang, Y.; Nuzzo, R. G.; Rogers, J. A. Transfer Printing Techniques for Materials Assembly and Micro/nanodevice Fabrication. *Adv. Mater.* **2012**, *24*, 5284−5318.
(29) Choi, M. K.; Yang, J.; Kang, K.; Kim, D. C.; Choi, C.; Park, C.; Kim, S. J.; Chae, S. I.; Kim, T.-H.; Kim, J. H.; Hyeon, T.; Kim, D.-H. Wearable Red−green−blue Quantum Dot Light-Emitting Diode Array Using High-Resolution Intaglio Transfer Printing. *Nat. Commun.* **2015**, *6*, 7149.
(30) Kim, T.-H.; Cho, K.-S.; Lee, E. K.; Lee, S. J.; Chae, J.; Kim, J. W.; Kim, D. H.; Kwon, J.-Y.; Amaratunga, G.; Lee, S. Y.; Choi, B. L.; Kuk, Y.; Kim, J. M.; Kim, K. Full-Colour Quantum Dot Displays Fabricated by Transfer Printing. *Nat. Photonics* **2011**, *5*, 176−182.
(31) Kim, T.-H.; Chung, D.-Y.; Ku, J.; Song, I.; Sul, S.; Kim, D.-H.; Cho, K.-S.; Choi, B. L.; Kim, J. M.; Hwang, S.; Kim, K. Heterogeneous Stacking of Nanodot Monolayers by Dry Pick-and-Place Transfer and Its Applications in Quantum Dot Light-Emitting Diodes. *Nat. Commun.* **2013**, *4*, 2637.
(32) Lee, S.; Yoon, D.; Choi, D.; Kim, T.-H. Mechanical Characterizations of High-Quality Quantum Dot Arrays *via* Transfer Printing. *Nanotechnology* **2013**, *24*, 025702.
(33) Lim, J.; Jun, S.; Jang, E.; Baik, H.; Kim, H.; Cho, J. Preparation of Highly Luminescent Nanocrystals and Their Application to Light-Emitting Diodes. *Adv. Mater.* **2007**, *19*, 1927−1932.
(34) Bae, W. K.; Kwak, J.; Park, J. W.; Char, K.; Lee, C.; Lee, S. Highly Efficient Green-Light-Emitting Diodes Based on CdSe@ZnS Quantum Dots with a Chemical-Composition Gradient. *Adv. Mater.* **2009**, *21*, 1690−1694.
(35) Bae, W. K.; Nam, M. K.; Char, K.; Lee, S. Gram-Scale One-Pot Synthesis of Highly Luminescent Blue Emitting Cd 1− X Zn X S/ZnS Nanocrystals. *Chem. Mater.* **2008**, *20*, 5307−5313.
(36) Stouwdam, J. W.; Janssen, R. A. J. Red, Green, and Blue Quantum Dot LEDs with Solution Processable ZnO Nanocrystal Electron Injection Layers. *J. Mater. Chem.* **2008**, *18*, 1889.
(37) Zakhidov, A. A.; Lee, J.-K.; Fong, H. H.; DeFranco, J. A.; Chatzichristidi, M.; Taylor, P. G.; Ober, C. K.; Malliaras, G. G. Hydrofluoroethers as Orthogonal Solvents for the Chemical Processing of Organic Electronic Materials. *Adv. Mater.* **2008**, *20*, 3481−3484.
(38) Qian, L.; Zheng, Y.; Xue, J.; Holloway, P. H. Stable and Efficient Quantum-Dot Light-Emitting Diodes Based on Solution-Processed Multilayer Structures. *Nat. Photonics* **2011**, *5*, 543−548.
(39) Kim, J.-H.; Han, C.-Y.; Lee, K.-H.; An, K.-S.; Song, W.; Kim, J.; Oh, M. S.; Do, Y. R.; Yang, H. Performance Improvement of Quantum Dot-Light-Emitting Diodes Enabled by an Alloyed ZnMgO Nanoparticle Electron Transport Layer. *Chem. Mater.* **2015**, *27*, 197−204.
(40) Saboktakin, M.; Ye, X.; Oh, S. J.; Hong, S.-H.; Fafarman, A. T.; Chettiar, U. K.; Engheta, N.; Murray, C. B.; Kagan, C. R. Metal-Enhanced Upconversion Luminescence Tunable through Metal Nanoparticle-Nanophosphor Separation. *ACS Nano* **2012**, *6*, 8758−8766.
(41) Cho, K.-S.; Lee, E. K.; Joo, W.-J.; Jang, E.; Kim, T.-H.; Lee, S. J.; Kwon, S.-J.; Han, J. Y.; Kim, B.-K.; Choi, B. L.; Kim, J. M. High-Performance Crosslinked Colloidal Quantum-Dot Light-Emitting Diodes. *Nat. Photonics* **2009**, *3*, 341−345.
(42) Panthani, M. G.; Kurley, J. M.; Crisp, R. W.; Dietz, T. C.; Ezzyat, T.; Luther, J. M.; Talapin, D. V. High Efficiency Solution Processed Sintered CdTe Nanocrystal Solar Cells: The Role of Interfaces. *Nano Lett.* **2014**, *14*, 670−675.
(43) Lee, J.-S.; Kovalenko, M. V.; Huang, J.; Chung, D. S.; Talapin, D. V. Band-like Transport, High Electron Mobility and High Photoconductivity in All-Inorganic Nanocrystal Arrays. *Nat. Nanotechnol.* **2011**, *6*, 348−352.
(44) Kim, D. K.; Lai, Y.; Diroll, B. T.; Murray, C. B.; Kagan, C. R. Flexible and Low-Voltage Integrated Circuits Constructed from High-Performance Nanocrystal Transistors. *Nat. Commun.* **2012**, *3*, 1216.
(45) Kang, M. S.; Sahu, A.; Norris, D. J.; Frisbie, C. D. Size-Dependent Electrical Transport in CdSe Nanocrystal Thin Films. *Nano Lett.* **2010**, *10*, 3727−3732.

DOI: 10.1021/acsnano.5b06387
ACS Nano XXXX, XXX, XXX−XXX